

High Cycle Fatigue Properties and Fracture Behavior of Ti-5Al-5Mo-5V-1Cr-1Fe Titanium Alloy

Liu Yingying, Zhang Le, Shi Xiaonan, Xue Xihao

Xi'an University of Architecture & Technology, Xi'an 710055, China

Abstract: Under different stress concentration factors K_t and stress ratios R , the high cycle fatigue (HCF) properties and fracture morphologies of Ti-5Al-5Mo-5V-1Cr-1Fe (Ti-55511) forgings and bars in longitudinal orientation were studied at room temperature. The results show that both the fatigue strength of forgings and bars increases with the increasing stress ratio and decreases with the increasing stress concentration factor. The fatigue strength of forgings is 1.08–1.57 times greater than that of bars. There are primary α phase particles in the forgings, with more uniform distribution and smaller size. However, there exist residual casting primary α phase particles with the shape of bulk or strip in bars.

Key words: titanium alloy; fatigue; stress concentration factor; stress ratio

Ti-5Al-5Mo-5V-1Cr-1Fe (Ti-55511) titanium alloy is widely used in the manufacture of aircraft fuselages, wing, landing gear and other large load-bearing components for its strong toughness, high plasticity and excellent welding performance^[1-4]. Fatigue fracture is the main form of failure for these alloys. Therefore, it is very important to understand its fatigue properties for its safety and economic applications in the aerospace field^[5-8]. Many scholars have carried out some research on the fatigue behavior of Ti-55511 alloy^[9-13]. Wu et al^[9] and Shi et al^[12] studied the effects of microstructure types on fatigue properties of the Ti-55511 titanium alloy. Li et al^[10] investigated the low cycle fatigue behavior of Ti-55511 titanium alloy at room temperature. Shi et al^[11,13] studied the crack initiation behavior and the fatigue crack growth rates of Ti-55511 titanium alloy. Unfortunately, little work was systematically conducted by comparing the high cycle fatigue properties of Ti-55511 forgings with Ti-55511 bars.

In the present paper, under different stress concentration factors K_t and stress ratios R , the room temperature high cycle fatigue (HCF) properties and fracture morphologies of Ti-55511 alloy in longitudinal orientation were studied by comparing the forgings with bars. The research results can

provide reference to the forging process parameters of Ti-55511 alloy, and the required fatigue strength design data for its applications in the aviation industry.

1 Experiment

The materials used in the present experiment are Ti-55511 forgings and bars (continuously cast bar stocks), and their chemical composition and microstructure are shown in Table 1, 2 and Fig.1, respectively. The mechanical properties of forgings and bars are shown in Table 3. As shown in Fig.1a, the microstructure of forgings is of basketweave where the acicular α phases interweave with β phases as a shape of baskets. In Fig.1b, the microstructure of bars is bimodal mainly composed of the primary α phases of equiaxed and striped shapes and the transformed β phases.

Fatigue specimens are smooth specimens ($K_t=1$) and notched specimens ($K_t=3, 5$), and the dimensions of them are shown in Fig.2. The experiments were carried out under the stress concentration factors K_t of 1, 3 and 5, stress ratios R of 0.5 and -1 , loading frequency around 150 Hz. In the present paper, the value of the fatigue strength as the maximum stress corresponds to 2×10^6 cycles in the $S-N$ curves.

Received date: December 20, 2017

Foundation item: Natural Science Foundation of Shaanxi Province (2016KW-054)

Corresponding author: Liu Yingying, Ph. D., Associate Professor, School of Metallurgical Engineering, Xi'an University of Architecture & Technology, Xi'an 710055, P. R. China, Tel: 0086-29-82205097, E-mail: wflly7779@163.com

Copyright © 2018, Northwest Institute for Nonferrous Metal Research. Published by Elsevier BV. All rights reserved.

Table 1 Chemical composition of forgings (wt%)

Al	Mo	V	Cr	Fe	C	Si	Zr	O	N	H	Ti
5.64	5.24	5.03	1.01	0.89	0.009	0.053	<0.01	0.12	0.005	0.003	Bal.

Table 2 Chemical composition of bars (wt%)

Al	Mo	V	Cr	Fe	C	Si	Zr	O	N	H	Ti
5.48	5.28	5.05	1.02	0.88	0.013	0.017	0.01	0.12	0.017	0.001	Bal.

Fatigue tests were carried out at room temperature by JXG100 high-frequency fatigue testing machine. The microstructure of specimens were observed by GX51 OLYMPUS metallographic microscope. The fracture morphologies of specimens were observed by TESCAN VEGA3 scanning electron microscope (SEM).

2 Results and Discussion

2.1 S-N curves

S-N curves of forgings and bars under different stress concentration factors K_t and stress ratios R are shown in Fig.3 and 4, respectively. In Fig.3, it can be seen that the fatigue strength increases with increasing R and decreases with increasing K_t . The same tendency can also be seen in Fig.4.

Similar conclusions in the study of the effect of stress ratio on the fatigue properties of Ti-6Al-4V alloys have been obtained by Liu et al^[14]. In short, stress ratio and the stress concentration factor are two important factors that affect the fatigue properties. Both the fatigue strength of forgings and bars increases with the increasing stress ratio and decreases with the increasing stress concentration factor.

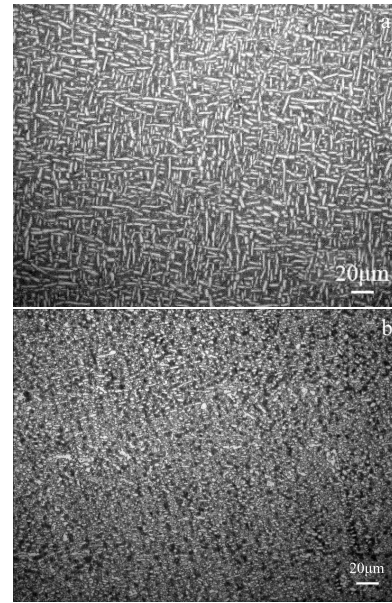


Fig.1 Microstructures of Ti-55511 alloy: (a) forgings and (b) bars

Table 3 Mechanical properties of forgings and bars

Material	Tensile strength/MPa	Yield strength/MPa	Elongation/%	Reduction of area/%	Elastic modulus/GPa
Ti-55511 forgings	1136	1085	12	37	114
Ti-55511 bars	1035	992	17	55	100

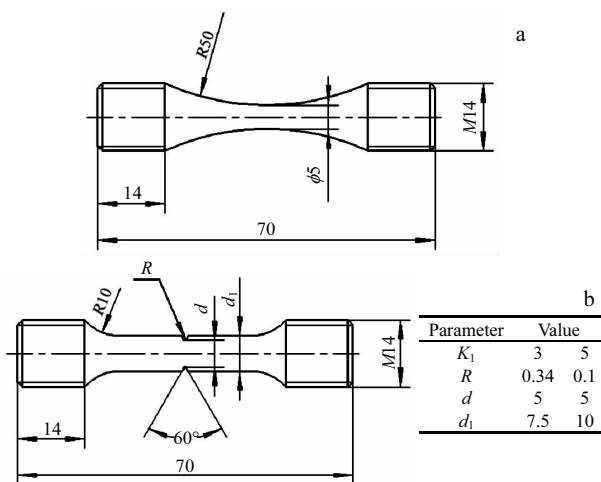


Fig.2 Dimensions of fatigue specimens: (a) smooth specimen and (b) notched specimen

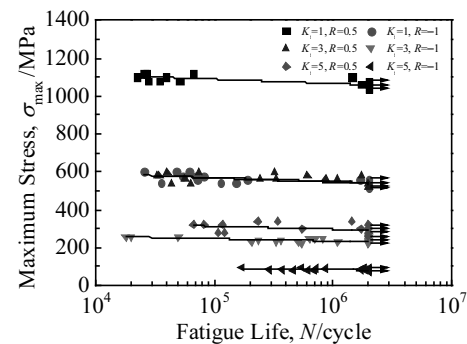


Fig.3 S-N curves of forgings under different stress concentration factors and stress ratios

S-N curves of forgings and bars under different stress concentration factors K_t and stress ratios R are shown in Fig.5.

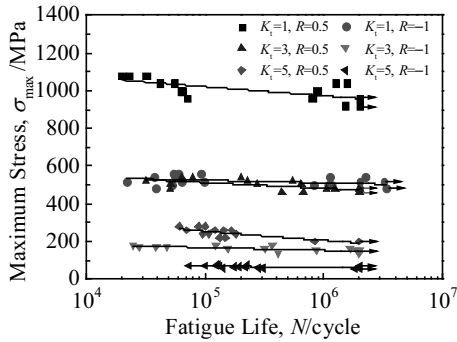


Fig.4 S-N curves of bars under different stress concentration factors and stress ratios

In Fig.5, the position of curves of forgings is higher than that of bars, which means the fatigue properties of forgings are better than those of bars. The fatigue strength of forgings and bars are shown in Table 4, where the fatigue strength of

forgings is 1.08~1.57 times greater than that of bars.

2.2 Fracture morphologies

The macroscopic and microscopic fracture morphologies of forgings are shown in Fig.6 and 7, respectively. In Fig.6, when the stress ratio $R=0.5$ the fracture surfaces are uneven (Fig.6a, Fig.6c and Fig.6e), which is corresponding to the ductile fracture and is beneficial for fatigue life. While the fracture surfaces are relatively flat in $R=-1$ (Fig.6b, Fig.6d and Fig.6f), which is corresponding to the brittle fracture and is bad for fatigue life. In addition, in Fig.6a and 6e there are hard primary α phase particles with small size and dispersed distribution. Fig.7a shows mixed features of tearing edges and dimples with uneven distribution. The cleavage steps can be seen in Fig.7b, the formation of which can be explained by the intersection of screw dislocations with the cleavage planes. Dimples with non-uniform size and tearing edges can also be seen in Fig.7c. Secondary cracks exist in Fig.7d. Dimples with shallow depth and uneven distribution can be seen in Fig.7e. Not only the transgranular cracking but also the intergranular fracture can be seen in Fig.7f.

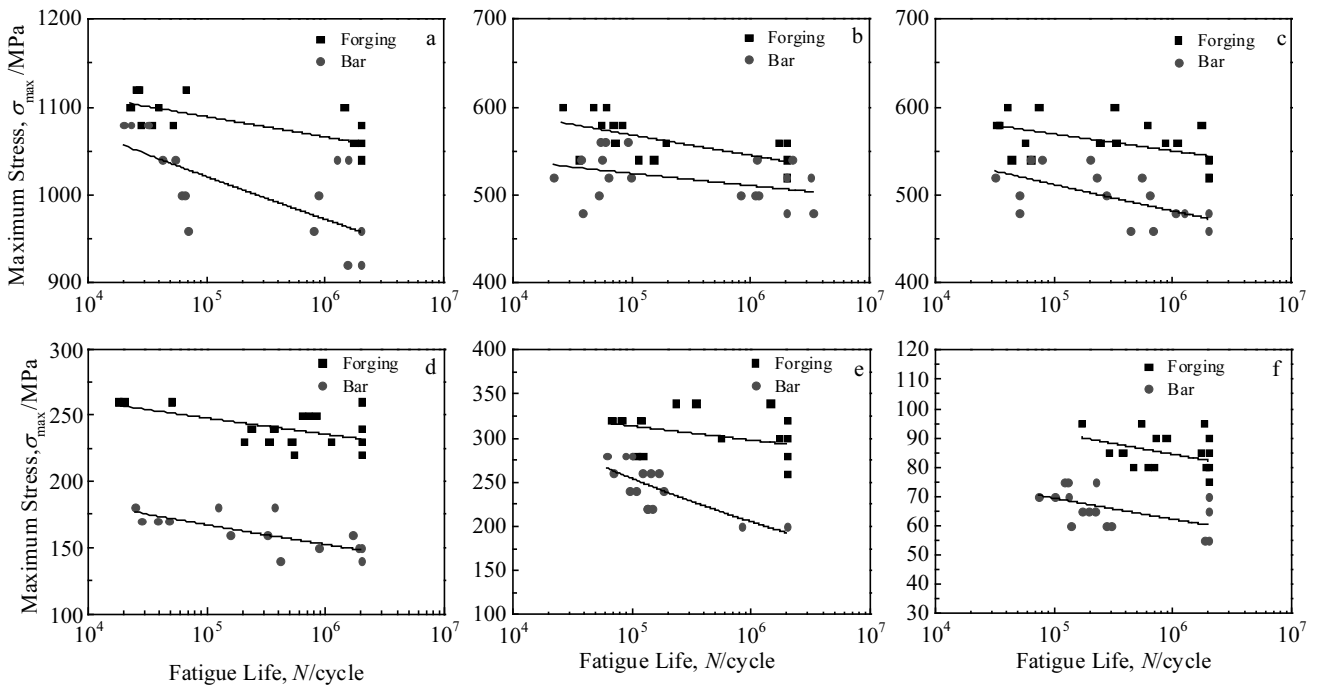


Fig.5 S-N curves of forgings and bars under different stress concentration factors and stress ratios: (a) $K_t=1, R=0.5$; (b) $K_t=1, R=-1$; (c) $K_t=3, R=0.5$; (d) $K_t=3, R=-1$; (e) $K_t=5, R=0.5$; (f) $K_t=5, R=-1$

Table 4 Fatigue strength of forging and bar at 2×10^6 cycles (MPa)

Material	$K_t=1$		$K_t=3$		$K_t=5$	
	$R=-1$	$R=0.5$	$R=-1$	$R=0.5$	$R=-1$	$R=0.5$
Ti-55511 forging	520	1040	220	520	75	260
Ti-55511 bar	480	920	140	460	55	200

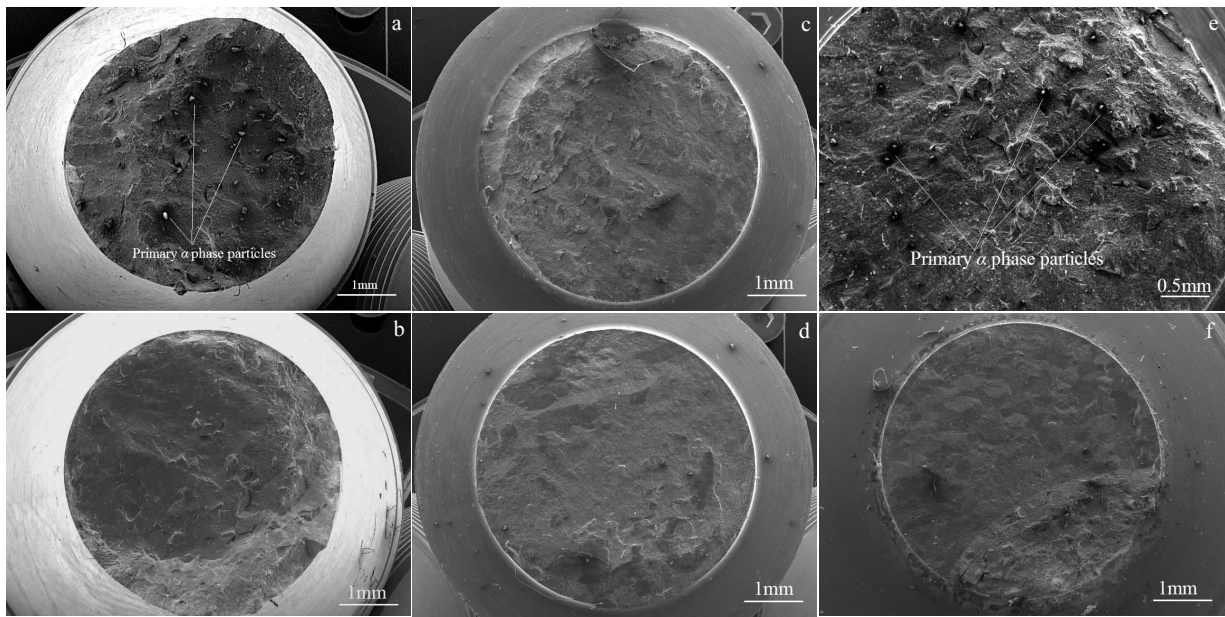


Fig.6 Macroscopic fracture morphologies of forgings: (a) $K_t=1$, $R=0.5$, $\sigma_{\max}=1080$ MPa, $N=5.13\times 10^4$ cycle; (b) $K_t=1$, $R=-1$, $\sigma_{\max}=540$ MPa, $N=3.56\times 10^4$ cycle; (c) $K_t=3$, $R=0.5$, $\sigma_{\max}=540$ MPa, $N=4.34\times 10^4$ cycle; (d) $K_t=3$, $R=-1$, $\sigma_{\max}=250$ MPa, $N=7.14\times 10^5$ cycle; (e) $K_t=5$, $R=0.5$, $\sigma_{\max}=280$ MPa, $N=1.08\times 10^5$ cycle; (f) $K_t=5$, $R=-1$, $\sigma_{\max}=80$ MPa, $N=4.65\times 10^5$ cycle

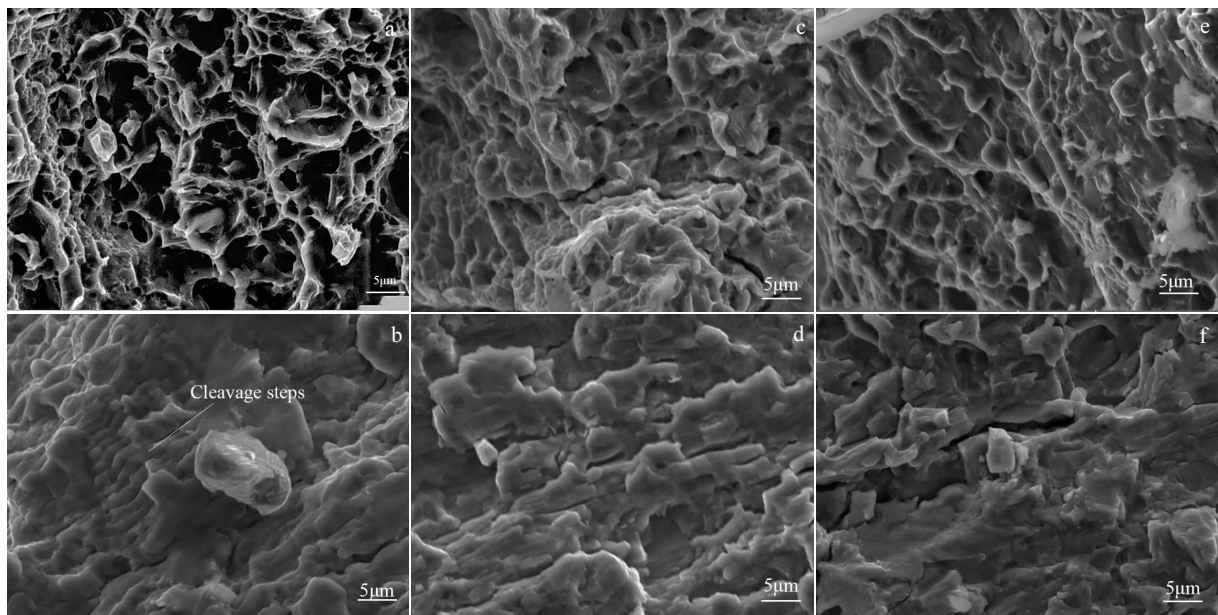


Fig.7 Micro fracture morphologies of forgings (crack propagation zone): (a) $K_t=1$, $R=0.5$, $\sigma_{\max}=1080$ MPa, $N=5.13\times 10^4$ cycle; (b) $K_t=1$, $R=-1$, $\sigma_{\max}=540$ MPa, $N=3.56\times 10^4$ cycle; (c) $K_t=3$, $R=0.5$, $\sigma_{\max}=540$ MPa, $N=4.34\times 10^4$ cycle; (d) $K_t=3$, $R=-1$, $\sigma_{\max}=250$ MPa, $N=7.14\times 10^5$ cycle; (e) $K_t=5$, $R=0.5$, $\sigma_{\max}=280$ MPa, $N=1.08\times 10^5$ cycle; (f) $K_t=5$, $R=-1$, $\sigma_{\max}=80$ MPa, $N=4.65\times 10^5$ cycle

When the stress ratio $R=0.5$ the main characteristic of the fracture is dimple fracture, which belongs to the ductile fracture (Fig.7a, Fig.7c and Fig.7e). When the stress ratio $R=-1$ the main characteristic of the fracture is cleavage fracture, which belongs to the brittle fracture (Fig.7b, Fig.7d

and Fig.7f). In addition, when the stress ratio $R=0.5$ the depth of dimples becomes shallower and the distributional uniformity of dimples becomes worse gradually with increasing the stress concentration factor K_t , which means a poorer fatigue performance. When the stress ratio $R=-1$ the

cleavage steps disappear gradually and the secondary cracks gradually appear with increasing the stress concentration factor K_t , which also means a poorer fatigue performance.

In addition, it can be seen from Fig.7 that the fracture morphology at higher fatigue life (10^5) is mainly characterized by cleavage or quasi cleavage (Fig.7d and Fig.7f). It shows

that the forgings mainly exhibit cleavage fracture rather than brittle fracture at higher fatigue life.

The macro and micro fracture morphologies of bars are shown in Fig.8 and 9, respectively. It can be seen from Fig.8a, Fig.8b and Fig.8e that there still remain longer primary α phase particles with the shape of bulks and strips. Under the

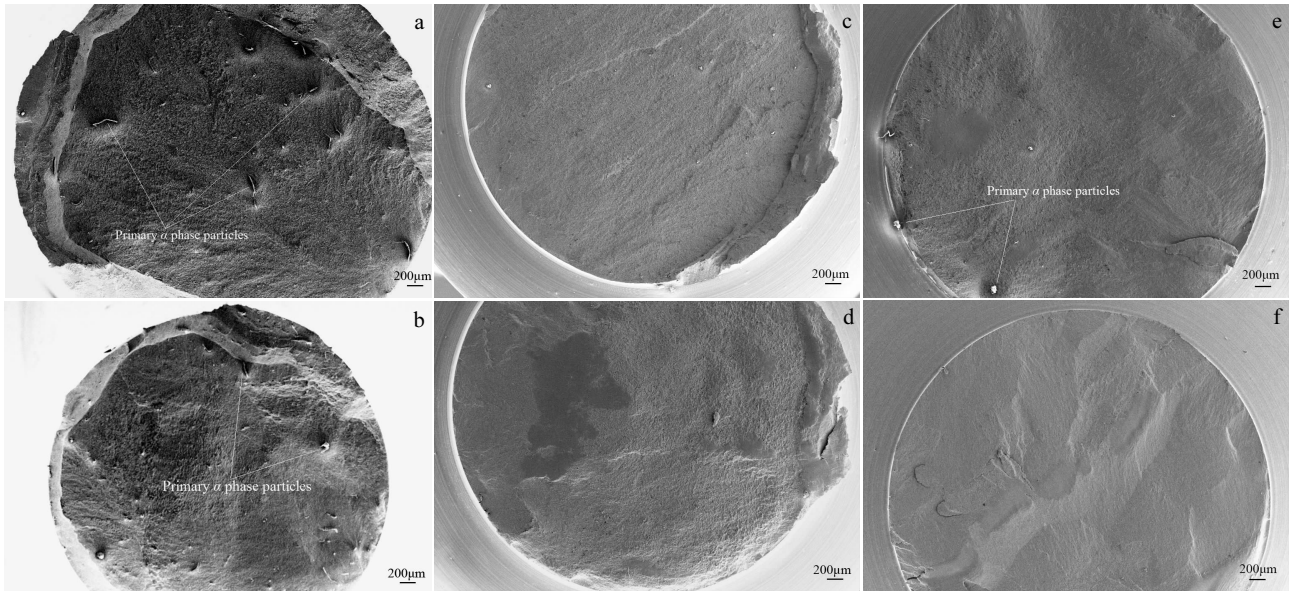


Fig.8 Macroscopic fracture morphologies of bars: (a) $K_t=1$, $R=0.5$, $\sigma_{max}=1080$ MPa, $N=2.0 \times 10^4$ cycle; (b) $K_t=1$, $R=-1$, $\sigma_{max}=560$ MPa, $N=5.38 \times 10^4$ cycle; (c) $K_t=3$, $R=0.5$, $\sigma_{max}=480$ MPa, $N=1.25 \times 10^6$ cycle; (d) $K_t=3$, $R=-1$, $\sigma_{max}=180$ MPa, $N=2.5 \times 10^4$ cycle; (e) $K_t=5$, $R=0.5$, $\sigma_{max}=260$ MPa, $N=1.67 \times 10^5$ cycle; (f) $K_t=5$, $R=-1$, $\sigma_{max}=55$ MPa, $N=1.85 \times 10^6$ cycle

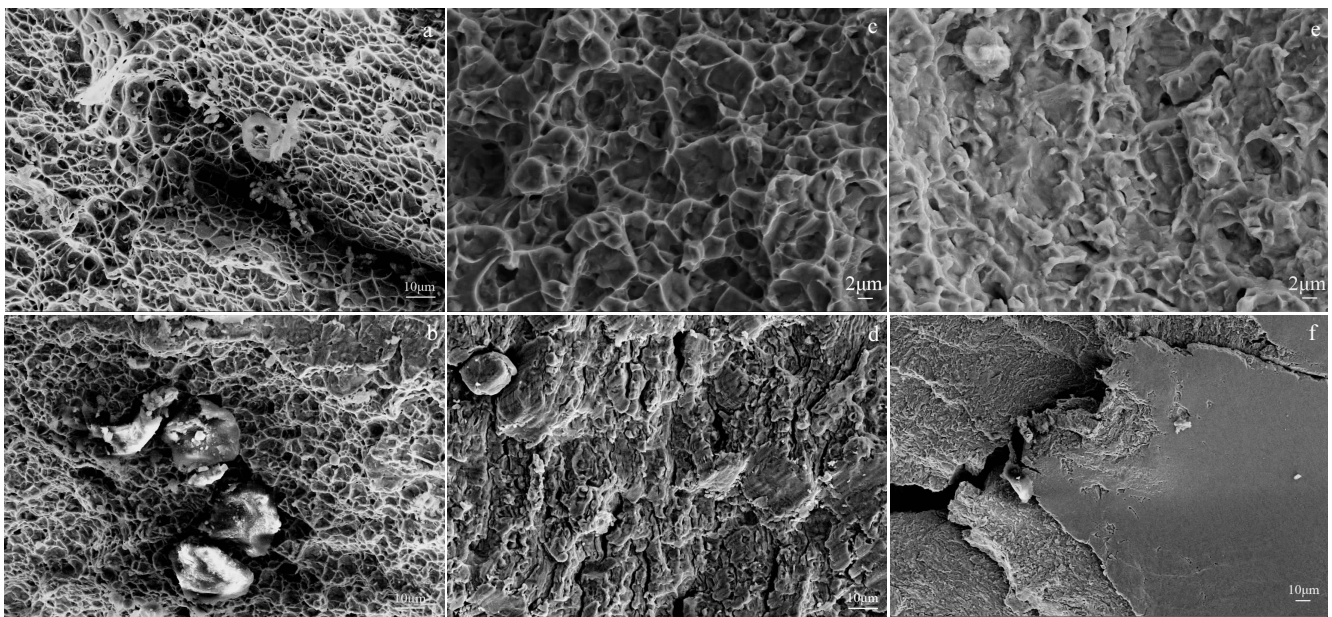


Fig.9 Micro fracture morphologies of bars (a~e: crack propagation zone, f: crack initiation zone): (a) $K_t=1$, $R=0.5$, $\sigma_{max}=1080$ MPa, $N=2.0 \times 10^4$ cycle; (b) $K_t=1$, $R=-1$, $\sigma_{max}=560$ MPa, $N=5.38 \times 10^4$ cycle; (c) $K_t=3$, $R=0.5$, $\sigma_{max}=480$ MPa, $N=1.25 \times 10^6$ cycle; (d) $K_t=3$, $R=-1$, $\sigma_{max}=180$ MPa, $N=2.5 \times 10^4$ cycle; (e) $K_t=5$, $R=0.5$, $\sigma_{max}=260$ MPa, $N=1.67 \times 10^5$ cycle; (f) $K_t=5$, $R=-1$, $\sigma_{max}=55$ MPa, $N=1.85 \times 10^6$ cycle

pull-tension stress, the hard particles cannot be coordinated with the matrix β and it is very easy to be separated from the matrix and becomes the obstacle to the progress of the dislocations. When the hard primary α phase particles are located on the edge of the specimens, the rate of cracks initiation will be very fast. However, if the primary α phase particles are located inside the specimens, a large number of accumulated dislocations will be necessary for cracks to initiate and break the matrix under the action of cyclic loading^[15,16].

Dimples with fine and uniform distribution can be seen in Fig.9a. The residual casting primary α phases with the shape of bulks and the small and uniform dimples are shown in Fig.9b. Dimples with uniform size and tearing edges can be seen in Fig.9c, which means that the bars still have a good plasticity at high fatigue life (10^6). Secondary cracks exist in Fig.9d. In Fig.9e, the difference in the size of dimples is large. Fig.9f shows the wear characteristics, and the cracks grow mainly along the β grain boundaries, which means that the bars have a great brittleness at high fatigue life (10^6). When $K_t=1, R=-1$ the bars show the characteristic of dimple fracture, rather than cleavage fracture as forgings, because there are fine equiaxed α phases in bars, and the equiaxed α phases will make the plasticity of specimens increase.

3 Conclusions

1) The fatigue properties of Ti-55511 forgings are better than those of Ti-55511 bars. And the fatigue strength of Ti-55511 forgings is 1.08~1.57 times greater than that of Ti-55511 bars.

2) There are primary α phase particles in the forgings with more uniform distribution and smaller size. However, there exist residual casting primary α phase particles with the shape of bulk or strip in bars.

3) When the stress ratio $R=0.5$, the microscopic fracture morphology of Ti-55511 forgings is mainly characterized by dimple fracture, which belongs to ductile fracture. When the

stress ratio $R=-1$, the microscopic fracture morphology of Ti-55511 forgings is mainly characterized by cleavage fracture, which belongs to brittle fracture.

References

- 1 Li Chao, Zhang Xiaoyong, Li Zhiyou et al. *Materials Science and Engineering A*[J], 2013, 573: 75
- 2 Li Chao, Zhang Xiaoyong, Zhou Kechao et al. *Materials Science and Engineering A*[J], 2012, 558: 668
- 3 Nyakana S L, Fanning J C, Boyer R R. *Journal of Materials Engineering and Performance*[J], 2005, 14(6): 799
- 4 Liang Houquan, Guo Hongzhen, Ning Yongquan et al. *Materials & Design*[J], 2014, 63: 798
- 5 Boyer R R, Briggs R D. *Journal of Materials Engineering and Performance*[J], 2005, 14(6): 681
- 6 Ivasishin O M, Markovsky P E, Matviychuk Y V et al. *Journal of Alloys and Compounds*[J], 2008, 457(1-2): 296
- 7 Ivasishin O M, Markovsky P E, Semiatin S L et al. *Materials Science and Engineering A*[J], 2005, 405(1-2): 296
- 8 Karasevskaya O P, Ivasishin O M, Semiatin S L et al. *Materials Science and Engineering A*[J], 2003, 354(1-2): 121
- 9 Wu G Q, Shi C L, Sha W et al. *Materials Science and Engineering A*[J], 2013, 575: 111
- 10 Li Zhen, Tian Xiangjun, Tang Haibo et al. *Transactions of Nonferrous Metals Society of China*[J], 2013, 23(9): 2591
- 11 Shi Xiaohui, Zeng Weidong, Xue Shikun et al. *Journal of Alloys and Compounds*[J], 2015, 631: 340
- 12 Shi Chenglong, Wu Guoqing, Sha Aixue et al. *Procedia Engineering*[J], 2012, 27: 1209
- 13 Shi Xiaohui, Zeng Weidong, Shi Chunling et al. *Materials Science and Engineering A*[J], 2015, 621: 143
- 14 Liu Xiaolong, Sun Chengqi, Hong Youshi. *Materials Science and Engineering A*[J], 2015, 622: 228
- 15 Klimova M, Zherebtsov S, Salishchev G et al. *Materials Science and Engineering A*[J], 2015, 645: 292
- 16 Li L X, Lou Y, Yang L B et al. *Materials & Design*[J], 2002, 23(5): 451

Ti-5Al-5Mo-5V-1Cr-1Fe 钛合金高周疲劳性能及断裂行为

刘莹莹, 张 乐, 史晓楠, 薛希豪
(西安建筑科技大学, 陕西 西安 710055)

摘 要: 研究了在不同应力集中系数 K_t 和应力比 R 下 Ti-5Al-5Mo-5V-1Cr-1Fe (Ti-55511) 锻件和棒材纵向的室温高周疲劳性能及断口形貌。结果表明: 锻件和棒材的疲劳强度均随应力比 R 的增大而增大, 随应力集中系数 K_t 的增大而减小。锻件的疲劳强度是棒材的 1.08~1.57 倍。锻件中存在初晶 α 相粒子, 其尺寸较小且分布较均匀; 棒材中则存在块状或条状的铸造残余初晶 α 相粒子。

关键词: 钛合金; 疲劳; 应力集中系数; 应力比

作者简介: 刘莹莹, 女, 1977 年生, 博士, 副教授, 西安建筑科技大学冶金工程学院, 陕西 西安 710055, 电话: 029-82205097, E-mail: wflly7779@163.com